Inorganic Chemistry

Article

Assignment of the Ferriheme Resonances of the Low-Spin Complexes of Nitrophorins 1 and 4 by ^{1}H and ^{13}C NMR Spectroscopy: Comparison to Structural Data Obtained from X-ray Crystallography

Tatiana Kh. Shokhireva,[†] Andrzej Weichsel,[‡] Kevin M. Smith,[§] Robert E. Berry,[†] Nikolai V. Shokhirev,[†] Celia A. Balfour,[†] Hongjun Zhang,[†] William R. Montfort,[†,‡] and F. Ann Walker*,[†,‡]

Departments of Chemistry and Biochemistry and Molecular Biophysics, The University of Arizona, Tucson, Arizona 85721, and Department of Chemistry, Louisiana State University, Baton Rouge, Louisiana 70803

Received July 27, 2006

In this work we report the assignment of the majority of the ferriheme resonances of low-spin nitrophorins (NP) 1 and 4 and compare them to those of NP2, published previously. It is found that the structure of the ferriheme complexes of NP1 and NP4, in terms of the orientation of the ligand(s), can be determined with good accuracy by NMR techniques in the low-spin forms and that angle plots proposed previously (Shokhirev, N. V.; Walker, F. A. *J. Biol. Inorg. Chem.* **1998**, *3*, 581−594) describe the angle of the effective nodal plane of the axial ligands in solution. The effective nodal plane of low-spin NP1, NP4, and NP2 complexes is in all cases of imidazole and histamine complexes quite similar to the average of the His-59 or -57 and the exogenous ligand angles seen in the X-ray crystal structures. For the cyanide complexes of the nitrophorins, however, the effective nodal plane of the axial ligand does not coincide with the actual histidine-imidazole plane orientation. This appears to be a result of the contribution of an additional source of asymmetry, the orientation of one of the zero-ruffling lines of the heme. Probably this effect exists for the imidazole and histamine complexes as well, but because the effect of asymmetry that occurs from planar exogenous axial ligands is much larger than the effect of heme ruffling the effect of the zero-ruffling line can only be detected for the cyanide complexes, where the only ligand plane is that of the proximal histidine. The three-dimensional structures of the three NP–CN complexes, including that of NP2–CN reported herein, confirm the high degree of ruffling of these complexes. There is an equilibrium between the two heme orientations (**A** and **B**) that depends on the heme cavity shape and changes somewhat with exogenous axial ligand. The **A:B** ratio can be much more accurately measured by NMR spectroscopy than by X-ray crystallography.

Introduction

The nitrophorins NP1−NP4 are a group of NO-carrying heme proteins found in the saliva of the blood-sucking insect *Rhodnius prolixus*, the "kissing bug".[1−5] NO is kept stable for long periods of time by binding it as an axial ligand to a ferriheme center.[1,3] Upon injection into the tissues of the victim, NO dissociates and diffuses through the tissues to the nearby capillaries to cause vasodilation and thereby allowing more blood to be transported to the site of the wound. At the same time, histamine, whose role is to cause swelling, itching, and initiation of the immune response, is

* To whom correspondence should be addressed. E-mail: awalker@u.arizona.edu.
† Department of Chemistry, The University of Arizona.
‡ Department of Biochemistry and Molecular Biophysics, The University of Arizona.
§ Louisiana State University.

(1) Ribeiro, J. M. C.; Hazzard, J. M. H.; Nussenzveig, R.; Champagne, D.; Walker, F. A. *Science* **1993**, *260*, 539−541.
(2) Champagne, D. E.; Nussenzveig, R. H.; Ribeiro, J. M. C. *J. Biol. Chem.* **1995***, 270*, 8691−8695.
(3) Walker, F. A.; Ribeiro, J. M. C.; Montfort, W. R. Novel NO-Liberating Heme Proteins from the Saliva of Blood-Sucking Insects. In *Metal Ions in Biological Systems, Vol. 36, Interrelations between Free Radicals and Metal Ions in Life Processes*; Sigel, H., Sigel A., Eds.; Marcel Dekker: New York, 1999; pp 619−661.
(4) Walker, F. A.; Montfort, W. R. The Nitric Oxide-Releasing Heme Proteins from the Saliva of the Blood-Sucking Insect *Rhodnius prolixus*. In *Advances in Inorganic Chemistry*; Mauk, A. G., Sykes, A. G., Eds.; Academic Press: San Diego, CA, 2001; Vol. 51, Chapter 5, pp 295−358.
(5) Walker, F. A. *J. Inorg. Biochem.* **2005**, *99*, 216−236.

released by mast cells and platelets of the victim. In the *Rhodnius* proteins, this histamine binds to the heme sites of the nitrophorins, hence preventing the insect's detection for a period of time.[6]

The *Rhodnius* proteins of the adult insect, named NP1−4 in order of their abundances in the insect saliva, have been investigated by a number of techniques[1,3,7−20] including spectroelectrochemistry,[7,9−11] NMR,[7,10,12] and EPR[7,13] spectroscopies. The solid-state structures of one or more ligand complexes of NP1,[7,14] NP2,[15,16] and NP4[17−22] have been determined by X-ray crystallography. The structures are unique for heme proteins, in that the heme is located at the open end of a β-barrel,[23] rather than in the more commonly observed largely α-helical globin[24] or 4-helix bundle[25−28] folds. The ferriheme molecule is bound to the protein via a histidine ligand, and the sixth coordination site is available to bind NO or other ligands.

(6) Ribeiro, J. M. C.; Walker, F. A. *J. Exper. Med.* **1994**, *180*, 2251−2257.

(7) Ding, X. D.; Weichsel, A.; Andersen, J. F.; Shokhireva, T. Kh.; Balfour, C.; Pierik, A. J.; Averill, B. A.; Montfort, W. R.; Walker, F. A. *J. Am. Chem. Soc.* **1999**, *121*, 128−138.

(8) Maes, E. M.; Walker, F. A.; Montfort, W. R.; Czernuszewicz, R. S. *J. Am. Chem. Soc.* **2001**, *123*, 11664−11672.

(9) Andersen, J. F.; Ding, X. D.; Balfour, C.; Champagne, D. E.; Walker, F. A.; Montfort, W. R. *Biochemistry* **2000**, *39*, 10118−10131.

(10) Shokhireva, T. Kh.; Berry, R. E.; Uno, E.; Balfour, C. A.; Zhang, H.; Walker, F. A. *Proc. Natl. Acad. Sci. U.S.A.* **2003**, *100*, 3778−3783.

(11) Berry, R. E.; Ding, X. D.; Shokhireva, T. Kh.; Weichsel, A.; Montfort, W. R.; Walker, F. A. *J. Biol. Inorg. Chem.* **2004**, *9*, 135−144.

(12) Shokhireva, T. Kh.; Shokhirev, N. V.; Walker, F. A. *Biochemistry* **2003**, *42*, 679−693.

(13) Astashkin, A. V.; Raitsimring, A. M.; Walker, F. A. *Chem. Phys. Lett.* **1999**, *306*, 9−17.

(14) Weichsel, A.; Andersen, J. F.; Champagne, D. E.; Walker, F. A.; Montfort, W. R. *Nature Struct. Biol.* **1998**, *5*, 304−309.

(15) Andersen, J. F.; Montfort, W. R. *J. Biol. Chem.* **2000**, *275*, 30496−30503.

(16) Weichsel, A.; Berry, R. E.; Zhang, H.; Walker, F. A.; Montfort, M. R. Manuscript to be submitted.

(17) Andersen, J. F.; Weichsel, A.; Balfour, C. A.; Champagne, D. E.; Montfort, W. R. *Structure* **1998**, *6*, 1315−1327.

(18) Weichsel, A.; Andersen, J. F.; Roberts, S. A.; Montfort, W. R. *Nature Struct. Biol.* **2000**, *7*, 551−554.

(19) Roberts, S. A.; Weichsel, A.; Qiu, Y.; Shelnutt, J. A.; Walker, F. A.; Montfort, W. R. *Biochemistry* **2001**, *40*, 11327−11337.

(20) Maes, E. M.; Weichsel, A.; Andersen, J. F.; Shepley, D.; Montfort, W. R. *Biochemistry* **2004**, *43*, 6679−6690.

(21) Kondrashov D. A.; Roberts S. A.; Weichsel, A.; Montfort, W. R. *Biochemistry* **2004**, *43*, 13637−13647.

(22) Maes, E. M.; Roberts, S. A.; Weichsel, A.; Montfort, W. R. *Biochemistry* **2005**, *44*, 12690−12699.

(23) Montfort, W. R.; Weichsel, A.; Andersen, J. F. *Biochim. Biophys. Acta* **2000**, *1482*, 110−118.

(24) Dickerson, R. E.; Geis, I. *Hemoglobin: Structure, Function, Evolution, and Pathology*; Benjamin/Cummings: Menlo Park, CA, 1983.

(25) Stryer, L. *Biochemistry*, 4th ed.; W. H. Freeman: New York, 1995; p 329.

(26) Lederer, F.; Glatigny, A.; Bethge, P. H.; Bellamy, H. D.; Matthew, F. S. *J. Mol. Biol.* **1981**, *148*, 427−448.

(27) Arnesano, F.; Banci, L.; Bertini, I.; Faraone-Mennella, J.; Rosato, A.; Barker, P. D.; Fersht, A. R. *Biochemistry* **1999**, *38*, 8657−8670.

(28) Finzel, B. C.; Weber, P. C.; Hardman, K. D.; Salemme, F. R. *J. Mol. Biol.* **1985**, *186*, 627−643.

(29) La Mar, G. N.; Walker, F. A. NMR Studies of Paramagnetic Metalloporphyrins. In *The Porphyrins*; Dolphin, D., Ed.; Academic Press: New York, 1979; Vol. IV, pp 61−157.

(30) Satterlee J. D. In *Metal Ions in Biological Systems*; Sigel, H., Ed.; Marcel Dekker: New York, 1987; Vol. 21, pp 121−185.

(31) Walker, F. A. Proton NMR and EPR Spectroscopy of Paramagnetic Metalloporphyrins. In *The Porphyrin Handbook*; Kadish, K. M., Smith, K. M., Guilard, R., Eds.; Academic Press: San Diego, CA, 2000; Chapter 36, Vol. 5, pp 81−183.

Of the spectroscopic techniques for characterizing heme proteins, proton NMR spectroscopy is one of the most important. Binding of even-electron donors, such as histamine, imidazoles, pyrazoles, or cyanide, to the NO-free forms of these proteins produces low-spin ($S = 1/2$) Fe(III) complexes.[7,10−13] The unpaired electron on the metal acts as a "beacon" that "illuminates" the protons in the vicinity of the metal, by causing shifts (called hyperfine, isotropic, or paramagnetic shifts) of the resonances from those observed in a diamagnetic protein. The two contributions to the paramagnetic shift are the contact (through bonds) and electron−nuclear dipolar or pseudocontact (through space) shifts; these are discussed in considerable detail elsewhere.[29−32]

The proton NMR spectra of the ferriheme center and nearby protein residues in the two paramagnetic forms of the four nitrophorins from *R. prolixus* have been investigated in detail in our laboratory. Early in this investigation it was found that of the four similarly structured proteins, NP2 provides by far the simplest NMR spectra. This is because unlike the other three nitrophorins, NP2 exhibits one predominant heme orientation,[12,15] and there are no chemical exchange cross-peaks observed in the NOESY spectra of this protein, unlike those of NP1 and NP4. Hence, we recently reported the assignment of the heme resonances of NP2 in its low-spin ($S = 1/2$) *N*-methylimidazole (NMeIm), imidazole (ImH), and 2-methylimidazole (2MeImH) complexes as well as those of the ligand-free, high-spin ($S = 5/2$) form.[10,12] Assignment of the heme resonances in both of these forms of the protein was made possible by the relative sharpness of the signals of the low-spin complexes, which allowed NOE cross-peaks to be detected for all heme substituents (even those whose resonances are buried in the large envelope of proton resonances from the protein). The low-spin Fe(III) complexes of NP1 and NP4 have only one heme methyl resonance resolved outside of the diamagnetic envelope, as shown below in this work. The high-spin ferriheme forms of these two show almost equal amounts of the two isomers that result from the two possible heme orientations, Chart 1.[33] Hence, in this work we have utilized specifically labeled hemins, where one or two of the methyls were deuterated, in order to fully assign the heme resonances of the axial ligand complexes of NP1 and NP4.

In this work we report the assignments of the majority of the ferriheme proton resonances in the low-spin paramagnetic forms of NP1 and NP4 as well as those of some previously unpublished axial ligand complexes of NP2. The pattern of hyperfine-shifted resonances observed for each of the proteins as a given ligand complex are then compared. The structure of NP2−CN has been solved and is compared to those of NP1−CN and NP4−CN.

(32) La Mar, G. N.; Satterlee, J. D.; De Ropp, J. S. Nuclear Magnetic Resonance of Hemoproteins. In *The Porphyrin Handbook*; Kadish, K. M., Smith, K. M., Guilard, R., Eds.; Academic Press: San Diego, CA, 2000; Chapter 37, Vol. 5, pp 185−298.

(33) Shokhireva, T. Kh.; Smith, K. M.; Berry, R. E.; Shokhirev, N. V.; Balfour, C. A.; Zhang, H.; Walker, F. A. *Inorg. Chem.* **2007**, *46*, 170−178.

Chart 1
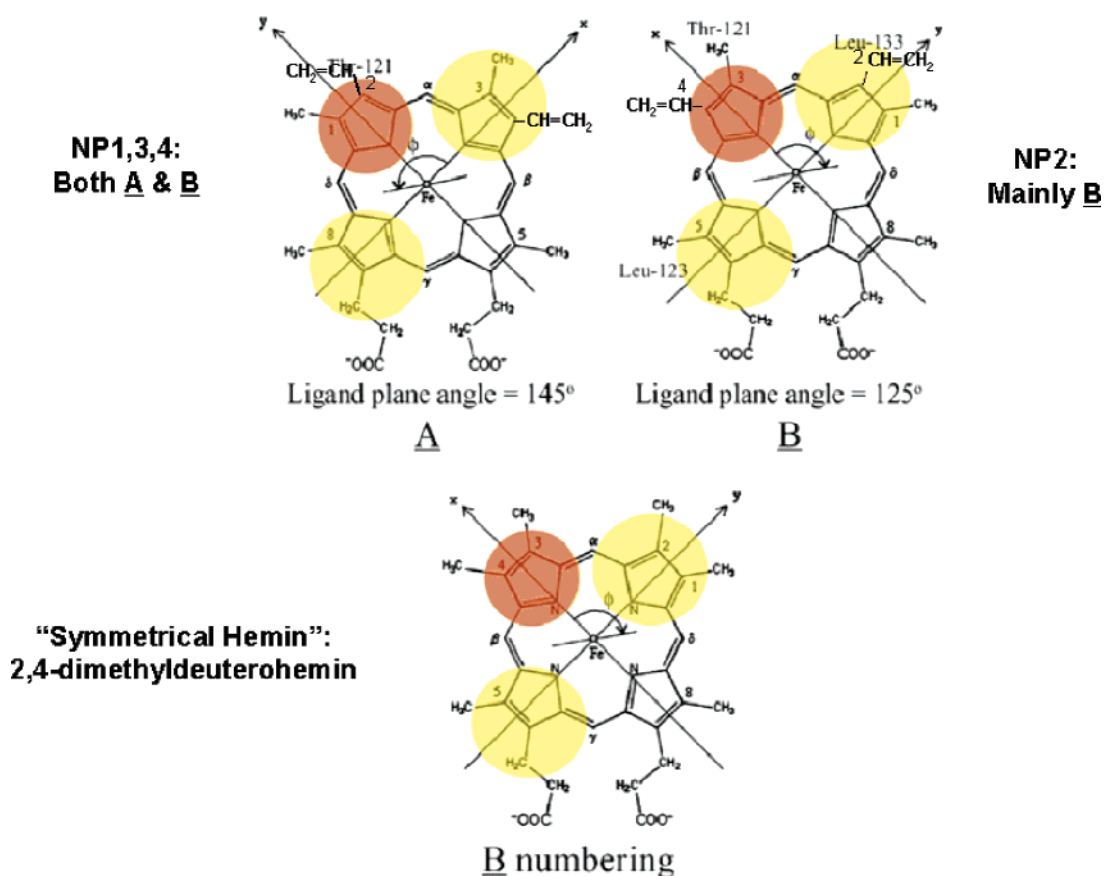
Experimental Section

Sample Preparation. The nitrophorin proteins NP1, NP2, and NP4 were prepared as described previously[7,14,15] and were stored in lyophilized form at −80 °C until use. NMR samples consisted of 1−4 mM solutions of each of the proteins in D_2O containing 30 mM phosphate buffer at pH 7.0 (uncorrected for the deuterium isotope effect). To obtain the low-spin complexes, each high-spin NP protein was titrated with the desired ligand (cyanide, histamine, or imidazole) until the proton NMR signals in the 70−30 ppm region[33] had just disappeared. Concomitantly, these signals were replaced by much sharper signals in the 30−10 ppm region. Especially for the cyanide complexes, it was found to be extremely important not to add any more ligand than necessary to cause disappearance of the high-spin resonances, and in fact, less than a stoichiometric amount of cyanide was found to be necessary for EPR measurements to avoid formation of some of the bis-cyanide complex, which has lost its protein-provided histidine ligand. Specifically labeled protohemin IX-containing protein samples for NMR spectroscopy were prepared as described previously[33] and then titrated with the desired ligand, as described above. It was found that typically only about 80−90% of the protohemin originally present in the holoprotein could be removed, and thus these reconstitution experiments always left some residual protonated-methyl protohemin present in the samples. Later in this project it was found that the apoprotein could be refolded and purified in the absence of hemin,[10] and hence a few remaining labeled heme complexes were prepared by titrating the apoprotein with the desired labeled hemin dissolved in NaOD as described above.

EPR Spectroscopy. EPR spectra were obtained on frozen protein solutions containing each of the desired ligands, added as described above, at 4.2 K on a Bruker ESP-300E EPR spectrometer operating at X-band using 0.2 mW microwave power, 100 kHz modulation frequency and 2−4 G modulation amplitude. A Systron-Donner frequency counter was used to measure the microwave frequency for precise calculation of *g*-values.

NMR Data Collection. NMR spectra were collected over the temperature range 25−30 °C with the proton chemical shifts referenced to residual HOD. NOESY and HMQC spectra were obtained on a Bruker DRX-500 spectrometer operating at 500.03 MHz proton Larmor frequency. The ^1H-^{13}C HMQC experiments were recorded using a 5 mm inverse-detection probe with decoupling during acquisition. A recycle delay of 200 ms and refocusing time of 2.5 ms ($J = 200$) were used. The WEFT-NOESY experiments utilized 100 ms relaxation delay and 130 ms recovery-delay. The mixing time for the NOESY experiments was 23−40 ms. All 2D spectra were collected with 1024 or 2048 data points in t_2 and with 256−512 blocks in t_1 with 400−800 scans/block.

Crystallography. Crystals of the NP2−CN complex were obtained using the hanging drop method by combining 2 μL of protein solution containing NP2 in 20 mM sodium phosphate pH 6.7 and 20 mM KCN with 2 μL of precipitant solution containing 89% saturated sodium citrate and 100 mM Hepes pH 7.5 and equilibration with the precipitant solution in the well at room temperature. The square platelike crystals were briefly transferred to 90% saturated sodium citrate, 2 mM KCN and flash frozen in liquid nitrogen. Diffraction data were measured at SSRL, Stanford, beam-line 9-2 at 100 K temperature using 0.97946 Å wavelength X-rays and MAR 325 CCD detector. The intensities were processed with d*TREK[34] to a maximum resolution of 1.2 Å. The structure was built using difference Fourier methods and PDB entry 1PEE

---

(34) Pflugrath, J. W. *Acta Crystallogr.* **1999**, *D55*, 1718−1725.

as a starting model. Local rebuilding was done with program COOT.[35] Refinement with anisotropic temperature factors at the final steps was carried out using program REFMAC5 from the CCP4 package.[36] The Fe–CN distance was restrained during refinement to 2.0 Å. Crystallographic data and refinement statistics for NP2–CN are given in Supporting Information Table S1. The atomic coordinates and structure factors have been deposited in the Protein Data Bank with identification code 2HYS.

Results and Discussion

1. EPR Spectra of the Low-Spin Fe(III) Nitrophorin–Ligand Complexes. The EPR spectra of the imidazole and histamine complexes of the nitrophorins are all extremely similar, and examples of these spectra have been reported previously for NP1–histamine ($g = 2.92, 2.24, 1.52$)[13] and NP4–imidazole ($g = 3.02, 2.25, 1.46$).[11] The similarity in the spectra for a given ligand is highlighted if we compare the g-values of NP2–ImH measured in this work ($g = 3.03, 2.26,$ and 1.37) to those of NP4–ImH mentioned above. In both of these ligand complexes the spectra are typical "B Hemicrome" rhombic EPR spectra[37,38] and need no further discussion. On the other hand, the cyanide complexes have the "large g_{max}"[39] or highly anisotropic low-spin (HALS)[40] or Type I[41] shapes, an example of which is shown in Supporting Information Figure S1. These "large g_{max}" EPR spectra are also all very similar to each other, with resolved g-values of 3.35, 1.96, and (calculated from $\Sigma g^2 = 16$) 0.97. They are also fairly similar to that of met-Mb-CN reported previously ($g = 3.45, 1.89, 0.72$ (calc))[42] and measured in our laboratory ($g = 3.45, 1.88,$ and 0.75 (calc)). The rhombic splitting (rhombicity, V/λ)[43] calculated from the g-values is much smaller for the cyanide complex than for the histamine and imidazole complexes ($V/\lambda = 1.00$ as compared to 1.89 and 1.62, respectively), indicating that the cylindrical cyanide ligand dominates the splitting between the d_{xz} and d_{yz} metal orbitals, in comparison to the planar histamine and imidazole ligands, while the average ligand field strength (tetragonality, Δ/λ)[43] of all three axial ligands in combination with the protein-provided histidine is surprisingly similar ($\Delta/\lambda = 3.07$ as compared to 2.96 and 2.85, respectively).

2. Proton NMR Heme Substituent Resonance Assignments for the Nitrophorin–Imidazole Complexes. Addition of strong-field ligands such as imidazole (ImH), histamine (Hm), or CN^- to the high-spin ($S = 5/2$) Fe(III) centers of the nitrophorins[33] creates the low-spin Fe(III) state ($S = 1/2$), which is characterized by a smaller range of NMR– shifts (30–40 ppm) and much sharper resonances

than those of the high-spin forms of the same proteins. In Figure 1A the NMR spectra of the imidazole, histamine, and cyanide complexes of NP1 are shown. All of these show ^1H resonances from both isomers, all with **A:B** ratios similar to those observed for the high-spin forms[33] of each protein. These **A:B** ratios are summarized in Table 1 for all of the protein/ligand complexes investigated in this work, along with the orientation angles of the His-57, -59 imidazole plane for each as determined by X-ray crystallography[14,17−19] and the orientation of the effective nodal plane of the axial ligand-(s) as determined by NMR spectroscopy in this work and in the paper on the high-spin forms of NP1 and NP4.[33] The effective nodal plane orientations, and their relationship to the X-ray crystallographic data, are discussed below. As discussed for the high-spin forms of the nitrophorins,[33] the NMR spectra of the low-spin imidazole complexes of the pair NP1, NP4 as compared to NP2 also differ significantly, as shown in Figure 1B. Contrary to our early unpublished assumption based on preliminary 1D NMR spectra before the heme resonances were assigned,[7] the NMR spectra of deuterated methyl-labeled hemins confirm that only one heme methyl resonance of NP1–ImH, observed at 25 ppm for isomer **A** and 17 ppm for isomer **B** at 30 °C, Figure 2, is resolved outside the diamagnetic envelope, while the other three are buried in the diamagnetic region of the NMR spectrum that is dominated by protein resonances (−1 to 11 ppm). The peak at 13 ppm that was earlier thought to be a heme methyl resonance on the basis of its 3-proton intensity is not changed in intensity upon substitution of any of the deuterated hemins, as shown in Figure 2, and at other pH and temperature conditions this peak splits into several resonances of very similar chemical shift (not shown). The analogous peak of NP4–ImH also behaves in this manner. It is possible to assign essentially all of the heme resonances of the **A** and **B** heme orientational isomers of NP1–ImH and NP4–ImH by WEFT-NOESY techniques, as shown in Supporting Information Figure S2 for NP4–ImH. These assignments are included in Table 2.

From the high-resolution crystal structures of NP4 and several of its ligand complexes, it was found that both heme orientations exist, in an **A:B** estimated ratio of 1.5:1,[17] and this is approximately the case for NP4–ImH on the basis of the ^1H NMR spectra (Figure 1B), which show an **A:B** ratio of ~2:1. For NP1–ImH and NP2–ImH, whose NMR spectra have been investigated in the greatest detail, one dominant heme rotational isomer is observed by X-ray crystallography for NP2–ImH,[15,16] the **B** isomer, while based on the crystal structure of NP4–ImH[19] it is the **A** isomer that is favored for that complex. The crystal structure of NP1–ImH has not been reported, but that of NP1–histamine has; only the **A** orientation was reported for that complex,[14] although NMR spectra reported in this work show that the **A:B** ratio in solution is ~1:1.

For complete assignment of the heme resonances of NP2–ImH[12] the situation was much more favorable than it is for the NP1 and NP4 complexes because of the three resolved heme methyl resonances (Figure 1B) as well as the lack of chemical exchange cross-peaks in the NOESY/EXSY spectra

(35) Emsley, P.; Cowtan, K. *Acta Crystallogr.* **2004**, *D60*, 2126−2132.
(36) Collaborative Computational Project Number 4. The CCP4 Suite: Programs for Protein Crystallography. *Acta Crystallogr.* **1994**, *D50*, 760−763.
(37) Blumberg, W. E.; Peisach, J. *Adv. Chem. Ser.* **1971**, *100*, 271−291.
(38) Peisach, J.; Blumberg, W. E.; Adler, A. D. *Ann. N. Y. Acad. Sci.* **1973**, *206*, 310−327.
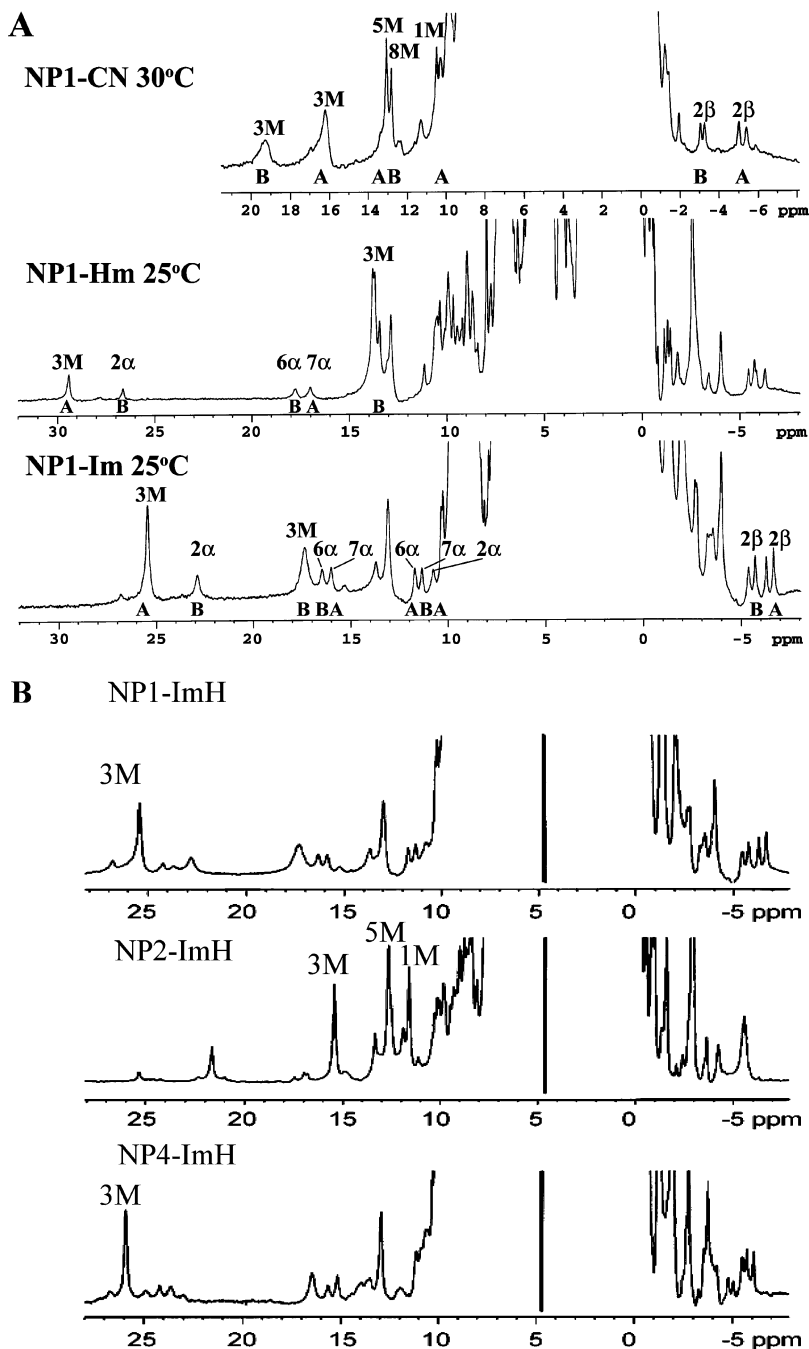(39) Walker, F. A.; Huynh, B. H.; Scheidt, W. R.; Osvath, S. R. *J. Am. Chem. Soc.* **1986**, *108*, 5288−5297.
(40) Migita, C. T.; Iwaizumi, M. *J. Am. Chem. Soc.* **1981**, *103*, 4378−4381.
(41) Walker, F. A. *Coord. Chem. Rev.* **1999**, *185−186*, 471−534.
(42) Thomson, A. J.; Gadsby, P. M. A. *J. Chem. Soc., Dalton Trans.* **1990**, 1921−1928.
(43) Taylor, C. P. S. *Biochim. Biophys. Acta* **1977**, *491*, 137−149.

Figure 1. A: 1D ^{1}H NMR spectra of the hyperfine-shifted resonances of three ligand complexes of NP1: top, CN$^-$ complex at 30 °C; middle, Hm complex at 25 °C; bottom, ImH complex at 25 °C. Note that the chemical shift scales are different in each spectrum. B: Comparison of the 1D ^{1}H NMR spectra of the hyperfine-shifted resonances of the ImH complexes of NP1, NP2, and NP4, recorded at 25 °C, 500 MHz.

of this protein. The plot of heme methyl chemical shifts vs histidine imidazole plane orientation for low-spin ferrihemes[44] is shown in Figure 3. This angle plot is based on the contact shifts that measure the calculated spin density distributions in the $e(\pi)$ orbital of the ferriheme for which the nodal plane of that orbital is coincident with the nodal plane of the axial ligand(s)[45] and the calculated pseudocontact shifts that depend on the orientation of the magnetic axes of

the heme, with counter-rotation of ligand and *x* or *y* magnetic axes.[46] Both of these contributions are related to the orientation of the nodal plane of the axial ligand, but with an angular dependence of different phase and much smaller magnitude for the pseudocontact (9%) than the contact shifts for the heme methyl resonances.[45] For quantitative separation of contact and pseudocontact contributions, subtraction of the diamagnetic shifts would be necessary; these are 3.51 ± 0.03 ppm,[47] a constant to the level of accuracy possible for

(44) It should be noted that this plot is 90° different in phase than shown in Figure 3 of the paper on the high-spin nitrophorins[33] because the orbital interactions that give rise to the contact shift are different.[12]

(45) Shokhirev, N. V.; Walker, F. A. *J. Biol. Inorg. Chem.* **1998**, *3*, 581–594.

(46) Shokhirev, N. V.; Walker, F. A. *J. Am. Chem. Soc.* **1998**, *120*, 981–990.

(47) Janson, T. R.; Katz, J. J. *J. Magn. Reson.* **1972**, *6*, 209–220.

Table 1. Crystallographic and NMR Angles (φ) of the Histidine Imidazole Plane and Exogenous Ligand for the A (B) Isomer and the Angle (α) for the Ruffling Zero Line Position and A:B Ratio for Some Nitrophorin Complexes

| protein, ligand | obtained from X-ray crystallography | | | | obtained from NMR spectroscopy | | |
	His φ_A $(\varphi_B)^a$	L φ_A $(\varphi_B)^a$	av^a	α_A $(\alpha_B)^a$	effective nodal plane^b	H or L dom.	A:B
NP1−NH₃	142.3 (127.7) I		142.3 (127.7)	179.7 (90.3)	139 (131)		~1:1
	135.9 (134.1) II		135.9 (134.1)	179.7 (90.3)	139 (131)		~1:1
NP1−CN	139.2 (130.8)		139.2 (130.8)	179.9 (90.1)	155 (117)	H59 + Ruf	1.2:1
NP1−ImH	c	c	c	c	130−133 (140−149)	H59 dominant	~1.1:1
NP1−Hm	139.8 (130.2)	104.5 (165.5)	122.2 (147.9)	179.4 (90.6)	132−134 (156−158)	H59 dominant	1:1.1
NP4−NH₃	131.2 (138.8)		131.2 (138.8)				
NP4−H₂O^d	133.1 (136.9)^d		133.1 (136.9)^d	173.2 (96.8)^d	137 (133)		1.1:1
NP4−CN	137.8 (132.2)		137.8 (132.2)	178.0 (92.0)	155 (117)	H59 + Ruf	1.2:1
NP4−ImH	130.1 (139.9)	114.6 (155.4)	122.4 (147.7)	167.8 (102.2)	130−133 (140−149)	H59 dominant	~2:1
NP4−Hm	134.2 (135.8)	104.1 (165.9)	119.2 (150.9)	173.3 (96.7)	132−134 (156−158)	H59 dominant	~1:1
NP2−NH₃(H₂O)	135.0 (135.0)		135.0 (135.0)		~136−137 (135)		1:8
NP2−CN	137.8 (132.2)		137.8 (132.2)	178.0 (92.0)	156−157 (114)	H57 + Ruf	1:4
NP2−ImH	134.4 (135.6)	112.5 (157.5)	123.5 (146.6)	175.8 (94.2)	(148−152)	ImH dominant	1:6
NP2−Hm	c	c	c	c	125−132 (156−157)	Hm dominant	1:4

^{a} Measured from the N$_{II}$−Fe−N$_{IV}$ axis, with positive numbers representing counterclockwise rotation. Taken from refs 14−19 and their corresponding PDB files (1NP1, 2NP1, 3NP1, 1X8P, 1D3S, 1IKJ, 1IKE, 1EQD, 1EUO, 2HYS, 1PEE, 1PM1). ^{b} Apparent nodal plane as measured from the ^{1}H NMR shifts of the heme methyls. ^{c} Structure not reported. ^{d} Crystallographic orientation inconsistent with ^{1}H methyl shifts.
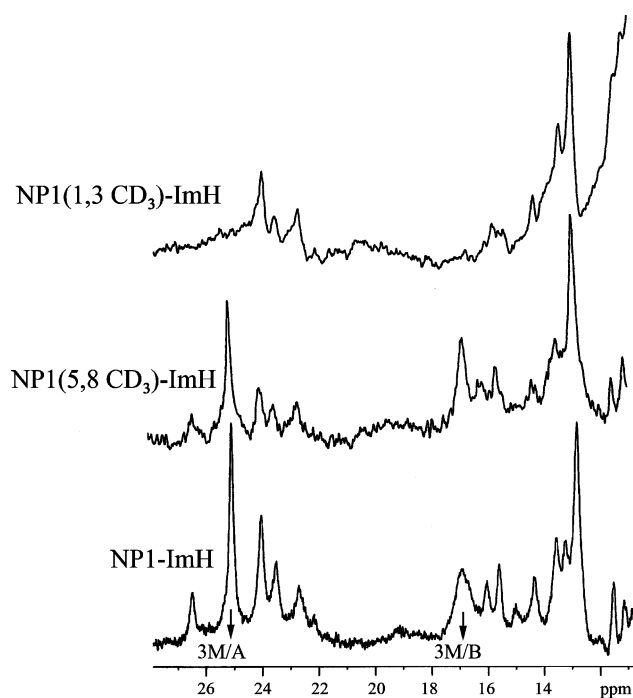
Figure 2. 1D ^{1}H NMR spectra of the high-frequency hyperfine-shifted resonances of native NP1−ImH (bottom) and its 5,8-(CD₃)₂- and 1,3-(CD₃)₂-hemin-substituted analogs (middle and top, respectively), measured at 30 °C, pH 7.0. With the assumption that the 1-methyl resonance should always have a smaller chemical shift than the 5-methyl,[45] the 3-CH₃ resonance is the only **A** isomer resonance resolved outside the protein envelope.

the chemical shifts of paramagnetic heme proteins. However, it should be noted that Figure 3 does not carry numbers on the chemical shift axis, because the aim of this work is not to separate contact and pseudocontact shifts quantitatively but rather *to consider the order and relative spacings of the heme methyl resonances*, since these alone are sufficient to define the approximate angle of the nodal plane of the histidine imidazole ligand. The plot of Figure 3 has been shown to be useful for analyzing the chemical shifts of the low-spin ferriheme resonances of a large number of heme proteins,[12,45,48] most recently to show that the solution structure of mouse neuroglobin is not the same as that seen

Table 2. Proton Chemical Shifts (in ppm) of the Imidazole Complexes of NP1 and NP4 and Comparison to Those of NP2, Measured at 30 °C, pH 7.0

|	NP1, isomer **A**	NP1, isomer **B**	NP4, isomer **A**	NP4, isomer **B**	NP2, isomer **B**
1Me	~2^a	8.9	1.7 (1.1)^b	9.4	11.5^c
3Me	25.1	17.0	25.7	16.4	15.6^c
5Me	~5^a	9.4	~5^a	10.3	12.5^c
8Me	9.9	~1^a	10.9	0.2	1.9
2V α	(13.3)^b	22.8	13.0	23.5	21.8^d
2V β	−5.8, −6.2^b	−5.0, −5.3	−5.5, −5.9	−5.3, −4.9	−5.9, −5.9^d
4V α	(8.9)^b		9.4		(6.1)^{b,c}
4V β					(1.2, 0.7)^{b,c}
6P α	11.5, 4.5	16.3, 7.9	11.1, 4.4	15.7, 8.6	12.9, 11.8^c
6P β	−3.8, −2.5	(−2.1, 0.0)^b	−2.7, −3.7	−2.0, 0.1	−1.2, −2.8^c
7P α	15.8, 7.6	(11.2, 4.6)^b	15.1, 8.2	10.9, 5.1	9.4, 4.9^c
7P β	0.0, −1.9	−3.8, −2.5		−2.6, −3.7	−2.8, −3.3^c
meso-α	−3.5	−3.1	−3.5	−3.0	−1.9^c
meso-β					7.7^c
meso-γ	−2.8	−2.9		−2.6	−3.9^c
meso-δ	5.6	6.0	5.1		9.9^c
av Me^e		~9.1	~10.8	9.1	10.4
Δ Me^f	~23	~16	24.0	16.2	13.7

^{a} Not assigned; approximate expected shift listed. ^{b} Assignment at 20 °C. ^{c} Taken from ref 12. ^{d} Corrected assignments for the 2-vinyl group (this work). ^{e} Average methyl resonance shift. ^{f} Spread of methyl resonances.

in the solid state by X-ray crystallography.[49] The complete assignment of the ^{1}H heme resonances of the NP2−ImH complex has been reported.[12] The three resolved heme methyl resonances of NP2−ImH are found at 14.9 (3Me), 13.5 (5Me), and 12.4 ppm (1Me) at 20 °C, Figure 1B; from the HMQC spectrum reported previously, the 8Me resonance is at −0.1 ppm.[12]

According to the deuterated hemin spectra of Figure 2, the single resolved heme methyl resonance of NP1−ImH is not the 5Me or the 8Me but rather is either the 1Me or 3Me, and using the rule of thumb that 5Me should have a larger chemical shift than 1Me[45] as well as the prediction of methyl resonance order as a function of the histidine imidazole plane orientation, Figure 3, which is known from X-ray structural data,[14] we can conclude that this is the 3Me resonance. The

(48) Altuve, A.; Silchenko, S.; Lee, K.-H.; Kuczera, K.; Terzyan, S.; Zhang, X.; Benson, D. R.; Rivera, M. *Biochemistry* **2001**, *40*, 9469−9483.
(49) Walker, F. A. *J. Biol. Inorg. Chem.* **2006**, *11*, 391−397.
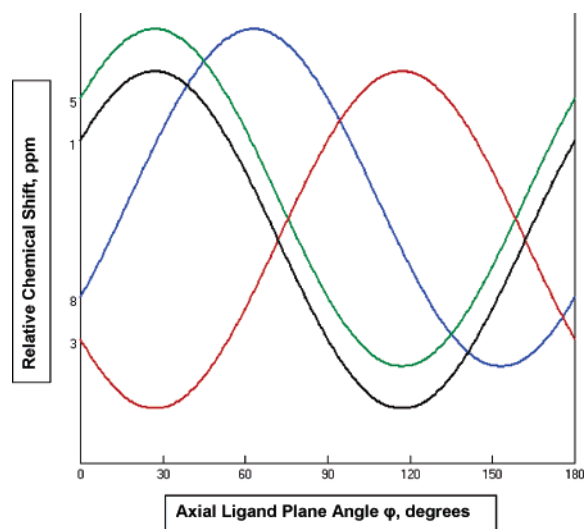
Figure 3. Relative chemical shift of the heme methyls vs ligand plane angle or effective ligand plane angle if two planar ligands are present, as calculated for low-spin ferrihemes.[45]

5-, 8-, and 1-methyl resonances of NP1−ImH are difficult to locate from the HMQC spectra of that protein because of the chemical exchange phenomena observed for this protein complex, to be discussed elsewhere, but it is clear that they are all buried in the diamagnetic protein envelope.

The 1D ^{1}H NMR spectrum of NP4−ImH is almost identical to that of NP1−ImH, although the chemical shifts are not exactly the same, as shown in Table 2 and in Figure 1B. The major difference between the ^{1}H NMR spectra of NP1−ImH and NP4−ImH is the intensity of the resonances that are assigned to the minor species, i.e., the **B** heme orientational isomer. As can be seen in Figure 1B, the ratio of the heme orientations **A:B** is ∼2:1 for NP4−ImH and ∼1:1 for NP1−ImH. In comparison to these two, the **A:B** heme orientation ratio for NP2−ImH is ∼1:8.[12] On the basis of the WEFT-NOESY cross-peaks observed for the 8Me and 1Me to the *meso*-δ-H (6.9 ppm), Supporting Information Figure S2, we assign the 8Me resonance of the **A** isomer at 30 °C to the resonance at 10.9 ppm and the 1M resonance to that at 1.7 ppm. It was not possible to assign the 5Me resonance unambiguously, but it must be at a chemical shift intermediate between those of the 8Me and 1Me resonances listed in Table 2.

The chemical shift of the single resolved 3Me heme resonance of NP1−ImH and NP4−ImH, with the other three methyl resonances buried in the protein envelope of the diamagnetic region of the spectrum having the order 8 > 5 > 1, places the orientation of the effective nodal plane of the two axial ligands at about 130−133° from the heme N−Fe−N axis connecting pyrrole rings C and A (crystallographic notation) or II and IV (NMR notation). This is because, according to the predictions of the effect of ligand plane orientation on the chemical shifts of the heme methyls,[45] Figure 3, it is only in the range of angles of about 128−134° that the other three methyl resonances should lie at chemical shifts small enough that they would not be found outside the protein resonance envelope. This is indeed close to the expected range of angles, as shown by the crystal

structures of NP4 and its ImH complex,[17,19] Table 1, for which the His-59 imidazole plane is oriented 130.1° counterclockwise of the N−Fe−N axis connecting pyrrole rings II and IV for isomer **A** (the major isomer for the imidazole complex), with the ImH plane oriented 15.5° clockwise of that, at 114.6°.[19] The average of these two is 122.4°, as compared to the effective nodal plane orientation determined from the NMR spectra, 130−133°. This is close to the orientation of the H59 imidazole plane of the **A** isomer of NP4−ImH,[19] suggesting that H59 plays a more important role in determining the effective nodal plane orientation than does the ImH exogenous ligand.

For NP2, the orientation of histidine and ImH imidazole planes is somewhat different, as summarized in Table 1. The nodal plane of His-57 has been shown by NMR studies of the high-spin protein to lie exactly along the β,δ-*meso* axis, with the **B** isomer most abundant in both high- and low-spin NP2.[12,33] The structure of NP2−ImH is in agreement with this, with the H57 imidazole plane lying at 135.6° from the N_{II}−Fe−N_{IV} axis for the **B** isomer, and the imidazole plane lying at 157.5° from that same axis (PDB file 1PEE),[16] a dihedral angle between axial ligand planes of 21.9°. The angular plot (Figure 3) for the ImH complex suggests an effective nodal plane orientation of the two ligands oriented at 148−152° clockwise from the N−Fe−N axis connecting pyrrole rings II and IV for the **B** isomer (Chart 1).[12] This is similar to the 146.6° average angle observed in the crystal structures.[18]

3. Proton NMR Heme Substituent Resonance Assignments for the Nitrophorin−Histamine (Hm) Complexes. Addition of histamine to NP1 and NP4 produces low-spin complexes having qualitatively similar ^{1}H NMR spectra to those of the imidazole complexes, except that the 3Me resonance is shifted to larger chemical shift (29.5 ppm as compared to 25.5 ppm for the imidazole complex, both at 25 °C), Figure 1A. Furthermore, the **B** heme orientation is slightly more abundant for NP1−Hm, **A:B** = 1:1.1. The complete NOESY/EXSY and HMQC spectra of NP1−Hm are shown in Supporting Information Figure S3. From the expanded region of the HMQC spectrum of NP1−Hm, shown in Figure 4, the order of heme methyl resonances for isomer **A** is 3Me > 8Me > 5Me > 1Me, while that for heme rotational isomer **B** is 3Me > 5Me > 1Me > 8Me. These orders and the relative spacings of the heme methyl resonances observed place the effective nodal plane angle near 132−134° for isomer **A** and near 156−158° for isomer **B**. From the X-ray crystal structure, the imidazole plane of His-59 of NP1−Hm is oriented 139.8° counterclockwise of the N_{II}−Fe−N_{IV} axis, while the imidazole plane of the histamine ligand in molecule I is oriented 104.5° counterclockwise of the N_{II}−Fe−N_{IV} axis (average angle 122.2°).[14] Because this average angle is smaller than that of the effective nodal plane angle (132−134°) we conclude that His-59 plays a somewhat more important role in determining the orientation of the nodal plane of the $e(\pi)$ orbital that is involved in spin delocalization to the porphyrin ring than does the histamine ligand. The same conclusion was reached in the ESEEM investigation of NP1−Hm.[13] (The reason for
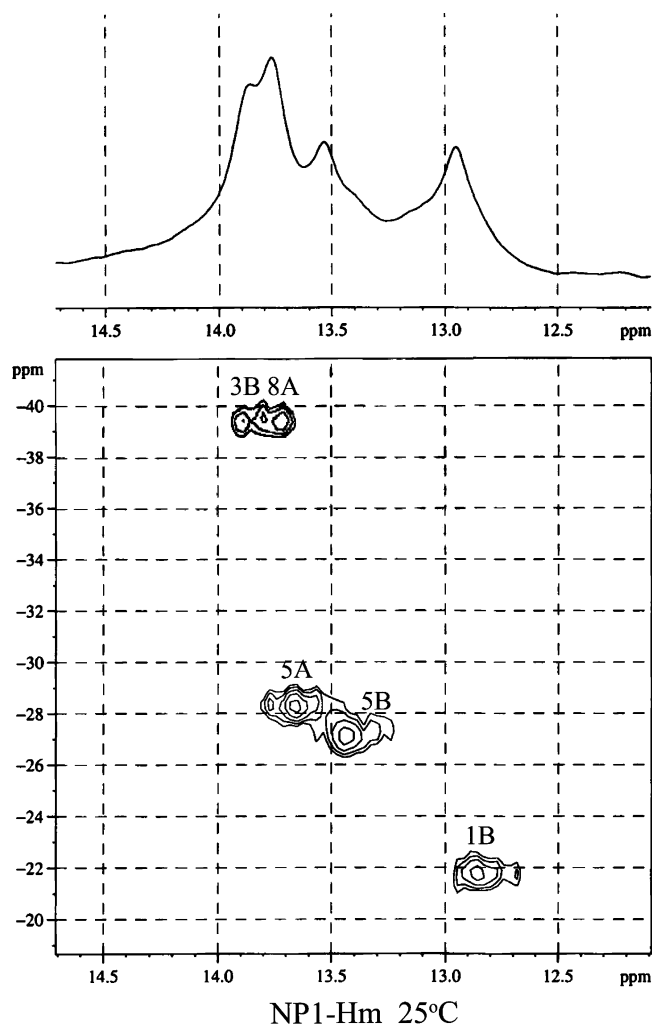
Figure 4. Expansion of $^{13}C/^1H$ HMQC spectrum of NP1−Hm from Supporting Information Figure S3 showing heme methyl resonances observed between 12.8 and 13.9 ppm.

one ligand contributing more strongly than the other, when both are imidazole donors, is that one ligand is engaged in stronger H-bond donation to some basic center than the other, which leaves that imidazole with a partial negative charge, i.e., it is more imidazolate-like than the other, and thus a stronger π donor.) In comparison to NP1−Hm, from the crystal structure of NP4−Hm[19] the imidazole ring of His-59 is oriented at 134.2° for isomer **A**, while the histamine imidazole plane is oriented at 104.1° for the **A** orientation, an average of 119.2°. The ^1H methyl shifts in the 1D NMR spectrum observed for the NP4−Hm complex suggest a similar effective nodal plane orientation of ∼118−124°, and thus in this case the axial ligands appear to contribute fairly equally to the effective nodal plane orientation.

The NMR spectra of NP2−Hm have not been reported previously. In this case, three heme methyl resonances are resolved outside the protein envelope, two closely spaced ones near 14 ppm and one at 13 ppm. Substitution of 5-CD₃-protohemin removes the first resonance (not shown), and thus the order of heme methyl resonances is 5 > 3 > 1 > 8 for NP2−Hm, with very close spacing of the three at 14−13 ppm. This close spacing suggests an effective ligand nodal plane orientation of 159−160°. The assignments are con-

firmed by the WEFT-NOESY and HMQC spectra shown in Figure 5. The X-ray crystal structure of NP2−Hm has not yet been reported, but it appears that as for the NP2−ImH complex, this is likely the angle of the histamine imidazole nodal plane. In comparison, the angles obtained for the **B** isomers of NP1−Hm and NP4−Hm by X-ray crystallography have this ligand at 165.5°[14] and 165.9°,[19] respectively. If this is the case, then the histamine imidazole ligand of NP2−Hm contributes more strongly to determining the effective nodal plane orientation than is the case for NP1−Hm and NP4−Hm. The chemical shifts of NP1−Hm and NP2−Hm at pH 7.0 are summarized in Table 3.

4. Structure of the NP2−Cyanide Complex. This structure is discussed before the presentation of the NMR data for the NP−CN complexes, in order that the structural characteristics may be used in the discussion of the NMR results. The asymmetric unit of the crystal contains one protein molecule and 171 water molecules, PDB file name 2HYS. All of the residues in the protein model are ordered except the N-terminal Met-0, part of the loop containing Gln-33 and Val-34, and the C-terminal Leu-179. The overall geometry of the protein is similar to that found in other NP2 structures,[16] for which the Protein Data Bank file names are included in footnote *a* of Table 1. The cyanide ligand is bound to heme in a linear arrangement, with the Fe−CN bond and the Fe−C−N bond angle of 1.99 Å and 175°, respectively, with cyanide slightly off the normal to the average heme plane in the direction of *meso-β*, and it forms an H-bond with a water molecule in the distal pocket. The heme group is well ordered in a single orientation (**B**) with well-defined vinyl and methyl groups. Two major components of the severely distorted heme plane are ruffling (−1.066 Å) and saddling (0.309 Å), which are very similar to those of the NP2−NO complex.[16] These distortions from planarity are significantly greater than those found previously for NP1−CN and NP4−CN, as calculated from the program "PDBTransform" created in our laboratory and available on our Web site,[50] shown in Figure 6, in agreement with the NMR data discussed below. Full description of the crystal structure and comparison to other nitrophorin structures will be presented elsewhere.[16]

5. Proton NMR Heme Substituent Resonance Assignments of the Cyanide Complexes of the Nitrophorins. Both 1- and 2-dimensional NMR techniques (1D NOE difference spectra, 2D COSY, TOCSY, NOESY, and ROESY spectra) have been extensively utilized to assign the hyperfine-shifted resonances of the heme in the cyanide-bound forms of ferriheme proteins,[32,45,51−66] where most, but

(50) Shokhirev, N. V.; Walker, F. A. PDBTransform. http://www.shokhirev.com/nikolai/programs/prgsciedu.html (accessed June, 2006).
(51) La Mar, G. N.; Smith, K. M.; Gersonde, K.; Sick, H.; Overkamp, M. *J. Biol. Chem.* **1980**, *255*, 66−70.
(52) La Mar, G. N.; de Ropp, J. S.; Smith, K. M.; Langry, K. C. *J. Biol. Chem.* **1981**, *256*, 237−243.
(53) Peyton, D. H.; La Mar, G. N.; Pande, U.; Ascoli, F.; Smith, K. M.; Pandey, R. K.; Parish, D. W.; Bolognesi, M.; Brunori, M. *Biochemistry* **1989**, *28*, 4880−4887.
(54) Emerson, S. D.; La Mar, G. N. *Biochemistry* **1990**, *29*, 1545−1556.
(55) De Ropp, J. S.; La Mar, G. N. *J. Am. Chem. Soc.* **1991**, *113*, 4348−4350.
(56) Alam, S. L.; Satterlee, J. D. *Biochemistry* **1994**, *33*, 4008−4018.
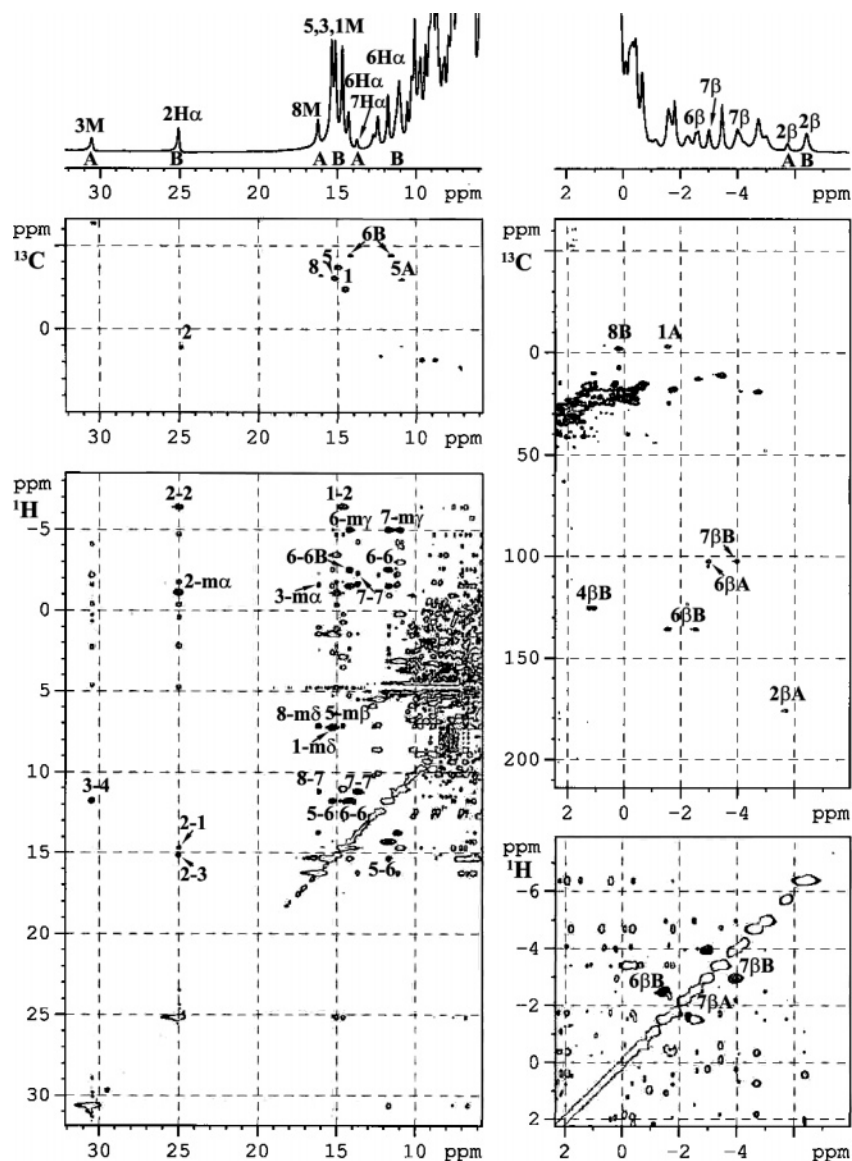
Figure 5. Left: Plot of the ^1H chemical shift range from 32 to 15 ppm for the 500 MHz $^{13}C/^1H$ HMQC spectrum of NP2−Hm recorded at 20 °C and the 500 MHz WEFT-NOESY spectrum of NP2−Hm recorded at 20 °C with a mixing time of 30 ms, showing correlations between *meso-α,β,γ,δ* and the 1,3,5,8-methyl, 2,4-vinyl, or 6,7-propionate resonances. Right: Plot of the same $^{13}C/^1H$ HMQC and WEFT-NOESY spectra of NP2−Hm over the +2 to −5 ^1H ppm region, showing correlations between 6α, 6β and between 7α, 7β protons.

not all, of the heme substituent resonances are found outside the diamagnetic envelope of the protein. In the present work,

(57) Banci, L.; Bertini, I.; Pierattelli, R.; Tien, M.; Vila, A. *J. Am. Chem. Soc.* **1995**, *117*, 8659−8667.
(58) Yamamoto, Y.; Suzuki, T. *Biochim. Biophys. Acta* **1996**, *1293*, 129−139.
(59) Zhang, W.; La Mar, G. N.; Gersonde, K. *Eur. J. Biochem.* **1996**, *237*, 841−853.
(60) Pierattelli, R.; Banci, L.; Turner, D. L. *J. Biol. Inorg. Chem.* **1996**, *1*, 320.
(61) Thanabal, V.; de Ropp, J. S.; La Mar, G. N. *J. Am. Chem. Soc.* **1997**, *109*, 265−272.
(62) De Ropp, J. S.; Mandal, P.; Brauer, S. L.; La Mar, G. N. *J. Am. Chem. Soc.* **1997**, *119*, 4732−4739.
(63) Gorst, C. M.; Wilks, A.; Yeh, D. C.; Ortiz de Montellano, P. R.; La Mar, G. N. *J. Am. Chem. Soc.* **1998**, *120*, 8875−8884.
(64) Caignan, G. A.; Deshmukh, R.; Wilks, A.; Zeng, Y.; Huang, H.; Moënne-Loccoz, P.; Bunce, R. A.; Eastman, M. A.; Rivera, M. *J. Am. Chem. Soc.* **2002**, *124*, 14879−14892.
(65) Li, Y.; Syvitski, R. T.; Auclair, K.; Wilks, A.; Ortiz de Montellano, P. R.; La Mar, G. N. *J. Biol. Chem.* **2002**, *277*, 33018−33031.
(66) Du, W.; Syvitski, R.; Dewilde, S.; Moene, L.; La Mar, G. N. *J. Am. Chem. Soc.* **2003**, *125*, 8080−8081.

CN^- has been utilized as an even-electron, diamagnetic substitute for NO in order to characterize the nitrophorins from *Rhodnius prolixus* in the paramagnetic low-spin ferriheme state. Unlike imidazole and histamine, the other two ligands that we have utilized and have discussed above, cyanide is a cylindrical anion that is expected (and found[67]) to bind along or close to the normal to the heme plane, and it thus has no ligand plane to affect the magnetic asymmetry of the heme complex.[45] Thus, in beginning this project, we expected that the cyanide complexes of NP1 and NP4 would provide excellent verification of the orientation of the proximal His-59 or -57 imidazole plane. However, we soon found that the cyanide complexes did not behave in manners predicted on the basis of the behavior of the high-spin aquo and low-spin imidazole and histamine complexes or the majority of the ferriheme cyanide protein complexes reported

(67) This work.

Table 3. ¹H and ¹³C Assignments of Heme Resonances of the Histamine Complexes of NP1 and NP2 at pH 7.0

	NP1−Hm, 25 °C				NP2−Hm, 20 °C			
	¹H, **A**	¹H, **B**	¹³C, **A**	¹³C, **B**	¹H, **A**	¹H, **B**	¹³C, **A**	¹³C, **B**
1M	−1.3	12.9	−1.6	−21.8	−1.5	14.6	−2.7	−24.1
3M	29.3	13.9	−64.1	−39.1	30.4	15.0	−63.6	−36.8
5M	13.7	13.4	−27.0	−28.2	~10.4ᵃ	15.3		−30.5
8M	13.8	0.2	−39.1	−5.4	16.0	0.2	−32.0	−5.4
2V α	10.7	26.5			11.1	24.9		22.2
2V β	−5.3, −5.5	−6.3, −5.9	175.8		−5.8	−6.5	176.4	
4V α	11.2	6.6			11.7	6.2		
4V β	0.5, −0.2	2.1, 1.8	159.4	125.8		1.2, 1.1		125.7
6P α	10.2, 2.5	17.6, 7.7	−29.6	−39.6	10.8, 3.7	14.1, 11.8		−43.6
6P β	−4.0, −2.7	0.2, −1.9	107.8		−3.0, −3.8	−1.6, −2.5		136.7
7P α	16.9, 7.5	10.2, 2.7	−39.9	−29.2	13.6, 11.2	10.9, 3.1		−29.5
7P β	0.3, −1.8	−2.7, −4.0	127.4		−2.3, −1.7	−4.1, −3.1		103.1
meso-α	−3.4	−3.0			−2.1	−1.0		
meso-β	7.9	6.8				7.2		
meso-γ	−2.7	−2.8			−4.2	−5.0		
meso-δ	6.3	7.0			7.1	11.0		
av. Meᵇ	13.8	10.2			~13.8	11.3		
Δ Meᶜ	30.6	13.7			31.9	15.1		

ᵃ Approximate chemical shift; resonance not assigned unambiguously. ᵇ Average methyl resonance shift. ᶜ Spread of methyl resonances.

previously.[32,45−66] Before discussing the differences in behavior, however, the NMR results obtained on the nitrophorin−cyanide complexes will first be presented.

In Figure 7 and Supporting Information Figure S4 are shown the WEFT-NOESY and HMQC spectra of NP1−CN and NP4−CN, respectively. As mentioned above, the **A:B** heme orientation ratio of the low-spin complexes depends on which ligand has been added. In the case of NP1−CN and NP4−CN, this ratio is close to 1.2:1 for both, and thus both isomers are present in reasonable concentration and both can be at least partially assigned. The HMQC map of both NP1−CN and NP4−CN exhibit six methyl resonances in the low shielding region of the ¹H spectrum, three for each isomer. The two most shifted resonances, observed in the NOESY maps and assigned as 3Me, are not observed in the HMQC maps, probably because of their shorter relaxation times that are possibly due to chemical exchange. Some dynamics that is incompletely averaged for the 3Me resonance of both NP1−CN and NP4−CN is suggested, although no dynamics is evident. The possible types of dynamics that could give rise to such incomplete averaging for the 3Me resonance do *not* involve cyanide on−off kinetics (the off-rate for cyanide is extremely slow, while the on-rate is extremely fast, which together yield a very large binding constant; R. E. Berry, unpublished work) but rather either changes in heme "seating" within the heme binding pocket or changes in the degree of ruffling of the heme. In this second case changes in the degree of ruffling would thus be a heme vibrational mode that is active on the NMR time scale and in order to result in incomplete averaging would have to be somewhat slower than that observed for the octaethylchlorin-bis-*tert*-butylisocyanide complex, published earlier, where the vibrational frequency was calculated by ADF methods to be 17 cm⁻¹ for saddling and 22 cm⁻¹ for ruffling.[68] However, these wavenumber values correspond to frequencies of 510 × 10⁶ and 660 × 10⁶ s⁻¹ (510 and

660 MHz), which are much too fast to affect the chemical shifts of resonances on the NMR time scale. Thus it is likely that changes in heme "seating", by just a few degrees, at frequencies close to the NMR time scale (for example between ~500 and 1500 Hz at 500 MHz for ¹H) account for the dynamics observed.

According to the plot derived for the dependence of heme methyl chemical shifts on axial ligand plane orientation, Figure 3, two different sets of methyl resonances are expected for the **A** and **B** isomers. Because cyanide binding does not change the symmetry of the heme complex by introducing a nodal plane, we expect that it will also not change dramatically the histidine plane orientation. Thus, the ratio $\varphi_A > \varphi_B$ deduced for the high-spin complexes should remain the same in the cyanide complexes. On the basis of this observation and the X-ray crystal structures of both NP1−CN[14] and NP4−CN,[19] we find that $\varphi_A > \varphi_B$ is the case for both, and thus isomer **B** has the 3Me resonance at larger chemical shift than isomer **A** (Figure 3). Using the NOESY spectra of Figure 7 and Supporting Information Figure S4 we have made a full assignment of the methyl resonances and most of the other heme substituent resonances of both isomers of both NP1−CN and NP4−CN as well as both isomers of NP2−CN discussed below. The chemical shifts are summarized in Table 4.

The effective nodal plane angles for the **A** and **B** isomers of NP1 derived from the order and relative spacings of the heme methyl resonances are 155° and 117°, respectively (average 136°), as summarized in Table 1. These angles are in poor agreement with the crystal structure of NP1−CN ($\varphi_A = 139.2°$, $\varphi_B = 130.8°$, respectively, average 135°),[14] NP4−CN ($\varphi_A = 137.8°$, $\varphi_B = 132.2°$, average 135°),[19] and NP2−CN ($\varphi_A = 137.8°$, $\varphi_B = 132.2°$, average 135°), with shifts predicted to be in the order 3 > 5 > 8 > 1 for **A** and 3 > 8 > 5 > 1 for **B**. Furthermore, the observed order of resonances 1 > 5 found for isomer **B** in each NP−CN complex violates the rule that the chemical shift of the 5-methyl should always be larger than that of the 1-methyl

(68) Cai, S.; Lichtenberger, D. L.; Walker, F. A. *Inorg. Chem.* **2005**, *44*, 1890−1903.
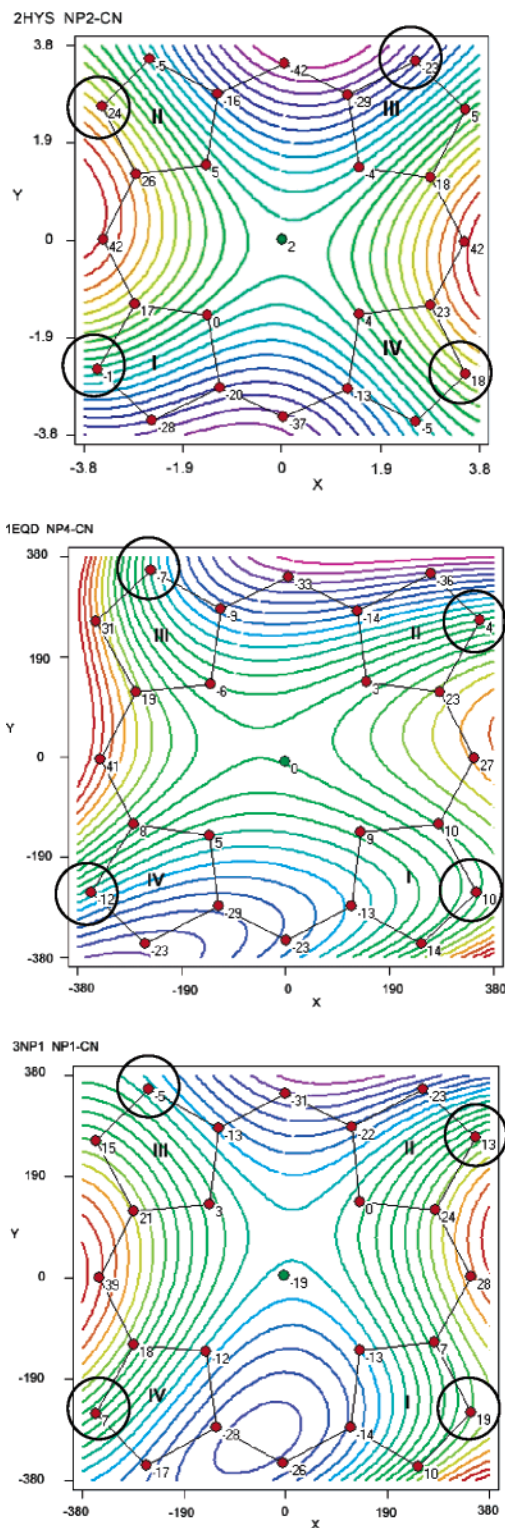
Figure 6. Plot of the deviations from the 24-atom mean plane (in 0.01 Å) and isodisplacement contours of NP2−CN as compared to NP4−CN and NP1−CN calculated from the program "PDBTransform".[50] Twenty-one contour colors vary from purple (−0.4 Å) to dark green (0.0 Å) to red (+0.4 Å). Positions where the 1,3,5,8-Me groups are bound are marked for the **B** orientation of NP2−CN and the **A** orientation of NP4−CN and NP1−CN.

because of the electron-withdrawing effect of the 2-vinyl substituent on 1Me.[45] This 5Me/1Me reversal may result from off-axis binding of the cyanide, such that there is a departure of the z magnetic axis from the heme normal due to a slight
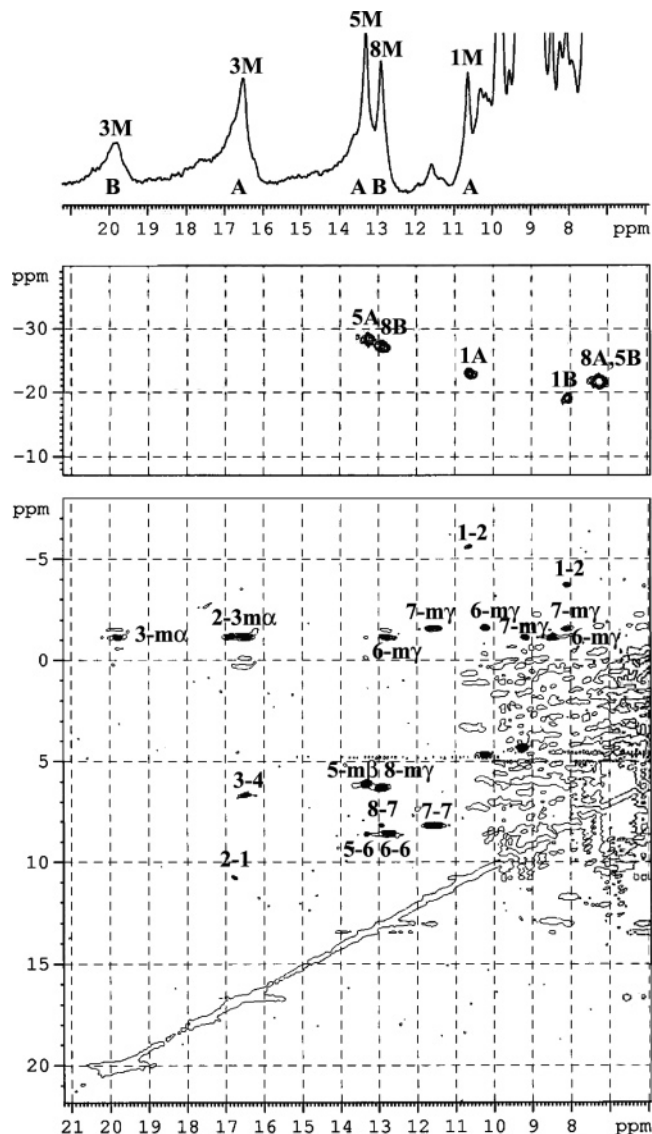
Figure 7. Plot of the ^{1}H chemical shift range from 21 to 6 ppm for the 500 MHz ^{13}C/^{1}H HMQC spectrum of NP1−CN recorded at 20 °C and the 500 MHz WEFT-NOESY spectrum of NP1−CN recorded at 20 °C with a mixing time of 30 ms. Methyl resonances 3B, 3A, 5A, 8B, and 1A are resolved outside the diamagnetic envelope in the 1D spectrum, and 1B, 8A, and 5B in the diamagnetic envelope are observed in the HMQC spectrum. The NOESY spectrum shows correlations among *meso*-α,β,γ,δ and the 1,3,5,8-methyl, 2,4-vinyl, and 6,7-propionate resonances.

tipping of the cyanide ligand from the heme normal.[65,69] For isomer **A** the departure from the heme normal would add to the difference in chemical shift of the 1Me and 5Me, while for isomer **B** it would subtract; thus it would be possible for 1Me to have a slightly larger chemical shift than 5Me. The crystal structure of NP4−CN indicates that the cyanide ligand leans slightly toward the β-*meso* position for isomer **A**,[19] and the β-*meso*-H shift is more positive than the δ-*meso*-H shift, a clear sign of off-axis cyanide binding.[65,69] For NP2−CN the lean of the cyanide ligand is very slightly toward pyrrole ring III (this work), and the α- and γ-*meso*-H shifts

(69) Emerson, S. D.; La Mar, G. N. *Biochemistry* **1990**, *29*, 1556−1566.
(70) Safo, M. K.; Walker, F. A.; Raitsimring, A. M.; Walters, W. P.; Dolata, D. P.; Debrunner, P. G.; Scheidt, W. R. *J. Am. Chem. Soc.* **1994**, *116*, 7760−7770.

Table 4. [1]H and [13]C Assignments of Heme Resonances of the Cyanide Complexes of NP1, NP4, and NP2 at pH 7.0

	NP1−CN, 20 °C				NP4−CN, 20 °C				NP2−CN, 30 °C			
	[1]H, **A**	[1]H, **B**	[13]C, **A**	[13]C, **B**	[1]H, **A**	[1]H, **B**	[13]C, **A**	[13]C, **B**	[1]H, **A**	[1]H, **B**	[13]C, **A**	[13]C, **B**
1Me	10.8	8.2	−22.7	−18.8	10.2	8.6	−22.2	−19.5	9.3	9.7	−18.2	−19.6
3Me	16.5	19.8			16.9	19.4			15.8	18.4	−34.9	−34.6
5Me	13.4	7.3	−27.9	−21.3	12.9	7.9	−27.6	−22.3	14.2	7.8	−20.5	−20.2
8Me	7.3	12.9	−21.3	−26.8	7.7	12.5	−22.8	−26.2	7.9	13.4	−20.2	
2V α	16.9	16.7			16.6	17.3			16.2	16.0		
2V β	−5.6, −6.1	−3.4, −3.6	193.7	186.0	−5.6, −6.1	−3.8, −3.5			−2.8, −3.5	−1.9, −2.1	180.0	178.5
4V α	6.7				6.6				6.6	7.4		
4V β	−0.2, −0.3		146.9						0.53, 0.47			125.8
6P α	12.9, 8.6	10.4, 4.7			12.2, 8.9	9.8, 5.6			12.1, 8.8	7.0, 7.5		−21.6
6P β					−1.9, −0.7	−1.9, −0.7				−0.4, −1.1		95.6
7P α	9.2, 4.2	11.6, 8.1			8.9, 5.1	11.1, 8.4				11.4, 8.1		−22.5
7P β	−1.4, −2.2	−0.8, −1.7			−1.9, −0.8	−2.0, −0.7				−0.8, −1.6		155.5
meso-α	−1.1	−1.1			−1.2	−1.3			1.2	2.3		
meso-β	6.3				5.9				6.0			
meso-γ	−1.5	−1.1			−1.3	−1.6				−1.8		
meso-δ	3.3	6.1			3.4	6.3				6.0		
av Me[a]	12.0	12.1			11.9	12.1			11.8	12.3		
ΔMe[b]	9.2	12.5			9.2	11.5			7.9	10.6		

[a] Average methyl resonance shift. [b] Methyl resonance spread.

differ from each other by about 4 ppm, while the β- and δ-*meso*-H resonances are at exactly the same chemical shift (6 ppm). Along with the order of heme methyl resonances, it is also observed that the chemical shifts are in general smaller in magnitude than those of the imidazole and histamine complexes as well as other ferriheme protein cyanide complexes.[32,45,48,51−66] For isomer **A**, the spread of the heme methyl resonances is 9.4 ppm for NP1−CN, 9.2 ppm for NP4−CN, and 7.9 ppm for NP2−CN (Table 4); the corresponding values for isomer **B** are each somewhat larger (13.6, 11.5, 10.6 ppm, respectively, Table 4). As will be discussed further below, the fact that the NP2 spread of heme resonances is smaller than those of NP1 and NP4 is consistent with the fact that the NP2 complex is the most ruffled of the three.

The 1D ^{1}H, WEFT-NOESY, and HMQC spectra of NP2−CN are shown in Figure 8, where it can be seen that the **B** heme rotational isomer again dominates, with the **A:B** ratio being about 1:6. In distinction to the high-spin form of NP2,[12] the apparent orientation of the His 57 imidazole plane is not along the β,δ-*meso* axis, for the two heme orientational isomers have different chemical shifts and different effective nodal plane orientations. From the pattern of shifts summarized in Table 4, using the same treatment as described above for NP1−CN and NP4−CN, it appears that for isomer **A** of NP2−CN the effective orientation of the nodal plane is at an angle of ∼155−157° counterclockwise from the $N_{II}−Fe−N_{IV}$ axis, while for isomer **B** it is ∼114−117° counterclockwise from the same axis. The solid-state structure of NP2−CN discussed above is indeed consistent with effective nodal plane orientations that are very similar to those of NP1−CN and NP4−CN discussed below.

The observed difference in effective nodal plane orientation upon binding CN⁻, in spite of the fact that it is a cylindrical ligand, shows that there is an additional factor that affects heme complex symmetry in addition to the orientation of the histidine nodal plane. We have concluded that this is heme distortion from planarity, which has been observed in the X-ray crystallographic structures of all

nitrophorin complexes; all nitrophorins have nonplanar hemes, with ruffling being the major distortion mode.[16−20] We have found that the heme is ruffled differently depending on the axial ligand bound to the Fe, not only in the deviations from the mean-plane but also in the orientation of the zero-level ruffling line α for that heme. This zero-level ruffling line is found by considering the deviations of the 24 ring atoms from the mean plane and calculating the orientation of the zero-deviation line using the program called "PDB-transform", available on our Web site.[50] In fact, there are actually two zero-level ruffling lines that are arranged at approximately 90° to each other, as shown in Figure 6 for NP2−CN, NP4−CN, and NP1−CN, the white X-shaped space in between the green or aqua contours that show the lowest level of deviation from planarity, with the white X centered fairly near the iron atom. As is evident from the three plots in Figure 6, the NP2−CN complex has the most *symmetrically* ruffled heme, with the white X passing closest to the four porphyrin nitrogens and the Fe in the center.

Which zero-ruffling line (which arm of the white X) should we consider? Actually, we should consider both. The white X-shaped space in between the green or aqua contours in Figure 6 shows which atoms of the heme are above the mean plane and which are below. For NP2−CN, 3Me and 5Me are slightly below the mean plane of the heme, while 1Me is slightly above and 8Me is significantly above the mean plane, while for NP4−CN and NP1−CN 1Me is significantly above the mean plane, 3Me is significantly below the mean plane, and 5Me and 8Me are somewhat above the mean plane of the heme. Although the contact shift may be affected by the ruffling of the heme, we cannot be sure about this; however, the pseudocontact shift is certainly affected by the above and below the mean plane of the heme positions of the methyl groups.

Since the z magnetic axis of the heme iron must be fairly close to the normal to the mean plane of the heme (but, however, shifted from that position by off-axis binding of the cyanide),[65,69] the magnitude and sign of the displacement of each methyl from the mean plane should significantly
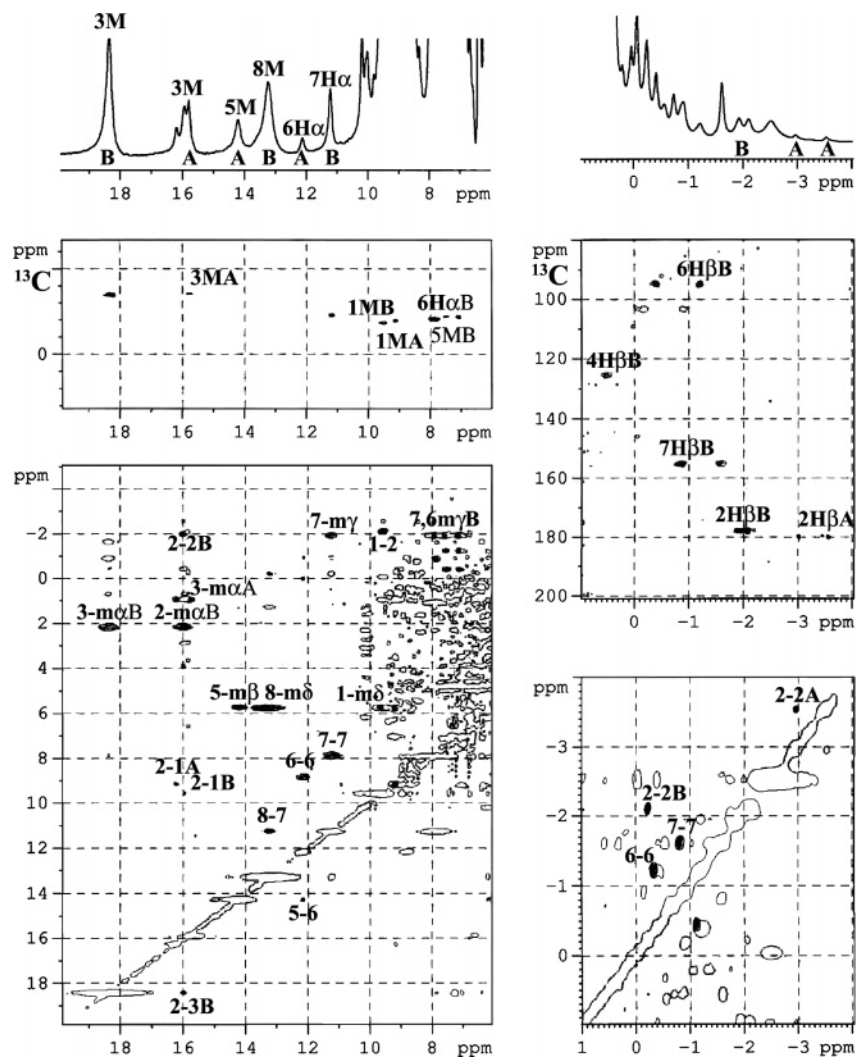
Figure 8. Left: Plot of the ¹H chemical shift range from 20 to 6 ppm for the 500 MHz ¹³C/¹H HMQC spectrum of NP2−CN recorded at 30 °C and the 500 MHz WEFT-NOESY spectrum of NP2−CN also recorded at 30 °C with a mixing time of 30 ms, showing NOE correlations between *meso*-α,β,γ,δ and the 1,3,5,8-methyl, 2-vinyl, or 6,7-propionate, the NOEs between 2-vinyl β resonances. Methyl resonances 3B, 3A, 5A, and 8B are resolved outside the diamagnetic envelope, and 1B, 1A, and 5B are seen in the HMQC spectrum. Right: Plot of the same ¹³C/¹H HMQC and WEFT-NOESY spectra of NP2−CN over the +2 to −4 ppm ¹H region, showing correlations between 2-vinyl-β-H, between 6β-H, and between 7β-H protons.

affect the pseudocontact shift experienced by each methyl group, for example for NP4, by shifting the 1Me, 5Me, and 8Me resonances in the positive chemical shift direction but the 3Me resonance in the negative chemical shift direction. This is exactly what would be expected if the effective nodal plane angle were somewhat larger than predicted by the orientation of the planar axial ligand (Figure 3), and thus by averaging the angle predicted by the orientation of the planar axial ligand with the angle predicted by the zero-ruffling line that corresponds to the "leg" of the white X that passes through the pyrrole rings at the top right and bottom left of each heme drawing of Figure 6, we obtain a predicted nodal plane orientation that is consistent with the observed angle (Table 1). This choice corresponds to choosing the zero ruffling line that passes through pyrrole rings II and IV for isomer **A** or I and III for isomer **B**. In general we find that the value of the zero ruffling line angle, α, chosen in this way, is fairly close to 0° or 180° for isomer **A** and to 90° for isomer **B**, whereas the histidine 57 or 59 imidazole plane orientation is fairly near 135° for both isomers of each

nitrophorin. In effect, the "zero ruffling line" adds another sin/cos dependence to the chemical shifts of the heme methyls that has the effect of shifting the phase of all four lines as compared to that shown in Figure 3. This shifting of phase can thus be simulated by averaging the effect of the nodal plane of the axial ligand, φ, and the orientation of the zero ruffling line as chosen above, α, to yield a larger apparent angle for the **A** isomer or a smaller apparent angle for the **B** isomer than would have been expected, based on the nodal plane orientation of the axial ligand alone.

If we consider these two angles, φ_A or φ_B and α_A or α_B, to contribute equally to determining the effective nodal plane for the cyanide complexes, then the calculated order of chemical shifts for the **A** isomers matches that observed and presented in Table 4, while the calculated order for the **B** isomers matches for the 3Me and 8Me resonances. However, this simple treatment cannot explain the reversal in the order of the 1Me and 5Me resonances, and the observation of this reversal is an indication of more complex effects such as off-axis cyanide binding, discussed above. For NP1−CN and

Table 5. Methyl Proton Shift Patterns for Histidine/Cyanide-Coordinated Ferriheme Proteins

protein	His-imidazole plane angle (°)	methyl shift order	methyl shifts (ppm)	spread (ppm)	av shift (ppm)	ref
sperm whale metMbCN	178	5 > 1 > 8 > 3	27.0, 18.6, 12.9, 4.8	22.2	15.8	51
elephant metMbCN	178	5 > 1 > 8 > 3	25.3, 16.5, 11.8, 5.9	19.4	14.9	69
G. japonica metMbCN	~178	5 > 1 > 8 > 3	25.1, 16.3, 10.5, 5.7	19.1	14.5	58
M. japonicas metMbCN	~178	5 > 1 > 8 > 3	25.9, 16.6, 10.2, 5.7	20.2	14.6	58
human metHb A CN α	159	5 > 1 > 8 > 3	20.9, 15.9, 8.7, 8.0	12.9[a]	13.4	72
human metHb A CN β	164	5 > 1 > 8 > 3	20.9, 14.7, 8.8, 8.1	12.6[a]	13.1	72
Glycera metHbCN	95	8 > 3 > 5 > 1	19.9, 18.8, 6.5, 0.6	19.2	11.5	56
Chironomus thumi thumi						
metHbCN III	~85	8 > 3 > 5 > 1	29.5, 22.2, 7.2, 3.4	26.1	15.6	59
metHbCN IV	~85	8 > 3 > 5 > 1	28.9, 21.4, 7.5, 3.9	25.0	15.4	59
Aplysia metMbCN	145−154	3 > 5 > 1 > 8	17.8, 15.7, 11.8, 9.9	7.9[a]	13.8	51
Scapharca metHbCN	~142	3 > 5 > 1 > 8	17.1, 12.7, 12.6, 7.8	9.3[a]	12.6	72
Dolabella metMbCN	~145	3 > 5 > 1 > 8	17.4, 15.1, 11.8, 10.2	7.2[a]	13.6	73
HRPCN	95	8 > 3 > 5 > 1	29.9, 25.1, 6.4, 2.9	27.0	16.1	58, 60
LiPCN	120	3 > 8 > 5 > 1	30.1, 20.5, 3.3, 0.8	29.3	13.6	57, 60
human heme-HOCN	125	3 > 8 > 5 > 1	19.6, 10.5, 9.0, 5.0	14.7[a]	11.0	63
C. diphtheriae heme-HOCN	125	3 > 8 > 5 > 1	19.2, 10.6, 8.5, 5.4	13.7[a]	10.9	63
P. aeruginosa heme-HOCN	35	5 > 1 > 8 > 3	27.7, 22.7, 19.0, 4.4	23.3	18.5	63
P. aeruginosa heme-HOCN alternate seating	105	3 > 8 > 5 > 1	24.6, 16.3, 5.4, 1.7	22.8	12.0	63
M80A cyt *c* CN	~45	8 > 5 > 1 > 3	22.5, 19.5, 15.4, 11.3	11.2[a]	17.2	74
MP8-CN	~45	8 > 5 > 1 > 3	23.2, 21.7, 16.4, 10.6	12.6[a]	18.0	75
horse cyt *c* CN	~45	5 > 8 > 1 > 3	23.1, 21.5, 16.6, 11.4	11.7[a]	18.2	76
NP1−CN **A**	139	3 > 5 > 1 > 8	16.7, 13.3, 10.8, 7.3	9.4[a]	12.1	TW[b]
B	131	3 > 8 > 1 > 5	20.9, 13.0, 8.2, 7.3	13.6[a]	12.4	TW[b]
NP4−CN **A**	138	3 > 5 > 1 > 8	16.9, 12.9, 10.2, 7.7	9.2[a]	11.9	TW[b]
B	132	3 > 8 > 1 > 5	19.4, 12.5, 8.6, 7.9	11.5[a]	12.1	TW[b]
NP2−CN **A**	138	3 > 5 > 1 > 8	15.8, 14.2, 9.3, 7.9	7.9[a]	11.8	TW[b]
B	132	3 > 8 > 1 > 5	18.4, 13.4, 9.7, 7.8	10.6[a]	12.3	TW[b]
protohemin-CN in DMSO		8 > 5 > 3 > 1	16.3, 15.9, 12.3, 10.3	6.3	13.6	83

[a] Heme methyl spread less than 15 ppm. [b] This work.

NP4−CN the average angle of the crystallographic histidine imidazole plane ($\varphi_A = 139.2°$, 137.8°, respectively) and the zero-line position ($\alpha_A = 179.9°$, 178.0°, respectively; average = 160° for **A** and 110° for **B** for NP1−CN, and 158° for **A** and 112° for **B** for NP4−CN) are in good agreement with the effective nodal plane angle. The fact that these values are somewhat larger for isomer **A** and smaller for isomer **B** than predicted by the effective nodal plane angles (155° and 117°, respectively) determined from the heme methyl shifts suggests that the zero-ruffling line position is of slightly smaller importance than the histidine nodal plane in determining the orientation of the effective nodal plane in these NP1,4-CN complexes or that the degree of ruffling in solution is greater than in the crystalline state. For NP2−CN the average angle of the crystallographic histidine imidazole plane ($\varphi_B = 132.2°$) and the zero-line position ($\alpha_B = 92.0°$) is 112.1° for **B**, while the NMR shifts predict an effective nodal plane of 114°, in very good agreement with the calculated angle.

In comparison to the nitrophorins, most of the ferriheme proteins for whose cyanide complexes the ^{1}H NMR spectra have been reported are those of myoglobins, hemoglobins, and peroxidases,[32,45,51−52,66] almost all of which have the histidine imidazole plane aligned along one or the other of the N_P−Fe−N_P axes. Such alignment of the imidazole plane "discourages" ruffling of the heme, whereas the orientation of H57(59) over the β- and δ-meso carbons, as in the *Rhodnius* nitrophorins, "encourages" ruffling. In addition, the nitrophorins also have two leucine residues in the distal pocket, L123 and L133 for NP1 and NP4[18,19] and L122 and L132 for NP2,[16] that are in van der Waals contact with the

heme and are believed to further encourage the heme to ruffle, with important consequences in terms of the stability of the Fe(III)−NO oxidation state.[10] As has been pointed out recently,[5] ruffling of a ferriheme tends to stabilize the d_{xz} and d_{yz} orbitals of the iron and, in the limit, leads to a change in the electron configuration of low-spin Fe(III) from the more common $(d_{xy})^2(d_{xz},d_{yz})^3$ to the less common $(d_{xz},d_{yz})^4$-$(d_{xy})^1$ configuration. This change in electron configuration usually brings about major changes in the g-values measured by EPR spectroscopy as well as major decreases in the proton chemical shifts of the β-pyrrole substituent resonances of the heme.[31] Both of these effects are aided by overlap between the half-filled d_{xy} orbital of iron and the porphyrin $2a_{2u}(\pi)$ molecular orbital.[31,70] This orbital has large spin density at the nitrogens and *meso*-carbons and very small spin density at the β-pyrrole carbons. Ruffling of the heme has important functional consequences for the nitric oxide complexes for which the cyanide complex is a model, in that strong ruffling of the heme should help to maintain the Fe(III) $(d_{xz},d_{yz})^4(d_{xy})^1$ − NO• electron configuration rather than the Fe(II) $(d_{xz},d_{yz})^4(d_{xy})^2$ − NO$^+$ electron configuration, thus helping to facilitate NO release.[5]

Thus, the spread of the heme methyl proton resonances of monocyano ferriheme proteins should be a measure of the degree of d_{xy} character of the metal unpaired electron and thus also of the degree of ruffling of the heme. In Table 5 are summarized the heme methyl proton chemical shifts for a number of ferriheme−cyanide complexes of heme proteins, including the three nitrophorins of this study. As is apparent, there are two classes of ferriheme−cyanide complexes: those having a spread of the heme methyl

resonances of 19.1−29.3 ppm and those having a spread of 7.2−14.7 ppm. The group with the larger spread of heme methyl resonances includes most of the metmyoglobin cyanides, except for those of *Aplysia* and *Dolabella*, the hemoglobins of *Scapharca* and human, but not lower organism hemoglobins, *Pseudomonas aeruginosa* heme−heme oxygenase-CN in both the normal and alternate seatings, but not human or *Corynebacterium diphtheriae* heme−heme oxygenase cyanides. By this criterion of large spread of the heme methyl resonances, we would expect these ferriheme−cyanide proteins to have planar hemes and pure $(d_{xy})^2(d_{xz},d_{yz})^3$ electron configurations in aqueous solution at ambient temperatures. On the other hand, *Aplysia*[71] and *Dolabella*[72] metmyoglobin cyanides, *Scapharca*[73] and human hemoglobin[72] cyanides, human[63] and *Corynebacterium diphtheriae* heme−heme oxygenase cyanide,[63] M80A cytochrome *c* cyanide,[74] microperoxidase-8-cyanide,[75] and horse cytochrome *c* cyanide[76] probably all have ruffled hemes, as do the nitrophorins of this study. In support of this statement, the structure of ferric *Aplysia limacina* Mb,[77] its CN⁻, N₃⁻, SCN⁻, F⁻, and imidazole complexes,[78] and several mutants where the mutated group is not near the heme binding pocket[79] as well as the *Scapharca inaequivalis* tetrameric HbII-CO[80] all show that the histidine imidazole plane is aligned closer to the *meso−meso* axis than to the N−Fe−N axis (150.5°, 145.2°, 152.6°, 152.7°, 145.8°, 147.9°, 152.7°, and 142.7°, respectively). And although the heme is modeled as being planar in these crystal structures, it is very likely that in solution a low-energy vibration can take the heme from a planar conformation to a ruffled or possibly a saddled one. Human metHbCN dimer has the His-imidazole plane closer to the N−Fe−N axis than these (α 164.9°, β 159.4°),[81] but these angles are still far from the N−Fe−N axis (0° or 180°) as compared to sperm whale, horse, or elephant Mb. The near-*meso−meso* orientation of the His-imidazole plane in each of these cases would "encourage" the ruffled conformation, and thus the NMR observation of very small spread of the heme methyl resonances of the cyanide complexes is consistent with a ruffled heme macrocycle at room temperature.

Ruffling leads to at least some degree of contribution from the $(d_{xz},d_{yz})^4(d_{xy})^1$ electron configuration.[70] Notably, as just

discussed for those for which structures are available, and as based on the order of heme methyl resonances for the other members of the latter group of proteins, have histidine imidazole planes oriented near either the β,δ- or the α,γ-*meso*-carbons, which "encourages" ruffling.[82] The degree of d_{xy} unpaired electron contribution does not have to be major, and in most cases is not, for all of the members of this second group of ferriheme cyanides have larger spreads of the methyl resonances than does protohemin bis-cyanide in DMSO-d_6 (6.3 ppm spread, Table 5),[83] where there is no ligand plane. But an increase in the degree of d_{xy} character has the effect of yielding a much smaller spread of the heme methyl resonances than the first group and thus suggests that the hemes of these complexes are quite ruffled. Interestingly, as discussed in section 1 above and shown in Supporting Information Figure S1, the EPR spectra of the nitrophorin−cyanide complexes are very similar to that of metMbCN, which indicates that at 4.2 K the electron configuration of both complexes is pure $(d_{xy})^2(d_{xz},d_{yz})^3$.[3] This means that the NP1−CN electron configuration changes with temperature. A similar change in electron configuration with temperature was observed for a model of heme oxygenase, [TPPFe-(OCH₃)(*t*-BuOO)]⁻, which also exhibited a $(d_{xy})^2(d_{xz},d_{yz})^3$ electron configuration with a planar heme at 4.2 K but a $(d_{xz},d_{yz})^4(d_{xy})^1$ electron configuration with a ruffled heme at ambient temperature.[84]

It is important to note that in the high-spin complexes,[33] the φ angle for the **A** isomer is larger than for the **B** isomer ($\varphi_A > \varphi_B$). We find this to be the same in the NP−CN complexes, as expected, because the cylindrical cyanide ligand should not change it. For the NP−ImH and NP−Hm complexes, however, this ratio changes to the opposite ($\varphi_A < \varphi_B$), as discussed above. This different behavior of cyanide as compared to the larger ligands may be due to space limitations for how larger ligands can sit at certain positions inside the heme cavity. Because neither the heme molecule nor the cavity is symmetrical, the heme adjusts its position in different ways for the **A** and **B** orientations depending on spin state and identity of the axial ligand, as discussed with regard to the high-spin forms of NP1 and NP2 and the two mutant proteins, NP1−Y28F and NP2−F27Y.[33]

6. Conclusions. In this work we have shown that the structure of the nitrophorin ferriheme complexes in terms of the orientation of the heme ligand(s) can be described with good accuracy by NMR techniques in the low-spin forms and that the angle plot shown in Figure 3 describes the angle of the effective nodal plane of the axial ligand(s) in solution. This angle plot is based on the calculated spin density distributions in the $e(\pi)$ orbital of the ferriheme for which the nodal plane of that orbital is coincident with that of the axial ligands[45] and in addition with the much smaller

(71) Wu, Y.; Basti, M.; Gambacurta, A.; Chiancone, E.; Ascoli, F.; La Mar, G. N. *Biochim. Biophys. Acta* **1996**, *1298*, 261−275.
(72) Kolczak, U.; Han C.; Sylvia, L. A.; La Mar, G. N. *J. Am. Chem. Soc.* **1997**, *119*, 12643−12654.
(73) Yamamoto, Y.; Suzuki, T. *Biochim. Biophys. Acta* **1993**, *1163*, 287−296.
(74) Banci, L.; Bertini, I.; Bren, K. L.; Cremonini, M. A.; Gray, H. B.; Luchinat, C.; Turano, P. *J. Biol. Inorg. Chem.* **1996**, *1*, 117−126.
(75) Low, D. W.; Gray, H. B.; Duus, J. Ø. *J. Am. Chem. Soc.* **1997**, *119*, 1−5.
(76) Brennan, L.; Turner, D. L. *Biochim. Biophys. Acta* **1997**, *1342*, 1−12.
(77) Bolognesi, M.; Onesti, S.; Gatti, G.; Coda, A.; Ascenzi, P.; Brunori, M. *J. Mol. Biol.* **1989**, *205*, 529−544.
(78) Conti, E.; Moser, C.; Rizzi, M.; Mattevi, A.; Lionetti, C.; Coda, A.; Ascenzi, P.; Brunori, M.; Bolognesi, M. *J. Mol. Biol.* **1993**, *233*, 498−508.
(79) Federici, L.; Savino, C.; Musto, R.; Travaglini-Allocatelli, C.; Cutruzzola, F.; Brunori, M. *Biochim. Biophys. Res. Commun.* **2000**, *269*, 58−63.
(80) Royer, Jr., W. E.; Heard, K. S.; Harrington, D. J.; Chiancone, E. *J. Mol. Biol.* **1995**, *253*, 168−186.
(81) Brucker, E. A. PDB file 1O1I, deposited 11/19/2002.
(82) Safo, M. K.; Gupta, G. P.; Walker, F. A.; Scheidt, W. R. *J. Am. Chem. Soc.* **1991**, *113*, 5497−5510.
(83) Barbush, M.; Dixon, D. W. *Biochem. Biophys. Res. Commun.* **1985**, *129*, 70−75.
(84) Rivera, M.; Caignan, G. A.; Astashkin, A. V.; Raitsimring, A. M.; Shokhireva, T. Kh.; Walker, F. A. *J. Am. Chem. Soc.* **2002**, *124*, 6077−6089.

magnetic anisotropy effects that result from the pseudocontact contribution to the paramagnetic shifts, which also depend on the orientation of the axial ligand. In this situation, however, we must allow for the possibility that one or the other axial ligand may be more important because it is a stronger π donor than the other. Unlike the case of mouse neuroglobin,[49] the effective nodal plane of the axial ligands of NP1, NP4, and NP2 is in all cases of imidazole and histamine complexes similar to those seen in the X-ray crystal structures. For the cyanide complexes of the nitrophorins, however, the effective nodal plane of the axial ligands does not coincide with the actual histidine imidazole plane position due to an additional source of asymmetry, the effect of heme ruffling and the orientation of the most important zero-ruffling line, as defined herein. Probably this effect exists for the imidazole and histamine complexes as well, but because the effect of asymmetry that occurs from axial ligand plane orientation is much larger for a planar ligand than the effect of heme ruffling we have only clearly detected the effect of the zero-ruffling line for the cyanide complexes, where the only ligand plane is that of the proximal histidine. It is also possible that the minor deviations observed for the effective nodal plane orientation from the average plane of the imidazole ligands (histidine, plus imidazole or histamine) is due to the effect of the zero-ruffling line rather than to one planar ligand contributing more strongly to the effective nodal plane orientation than the other.

There is an equilibrium between the two heme orientations (**A** and **B**), that depends not only on heme binding ability but also on the heme cavity properties such as cavity shape, size, and possibly other contributions as well. **A**:**B** ratio can be much more accurately measured by NMR spectroscopy than by X-ray crystallography.

Supporting Information Available: Figures **S1**−**S4**. This material is available free of charge via the Internet at http://pubs.acs.org.

IC061408L